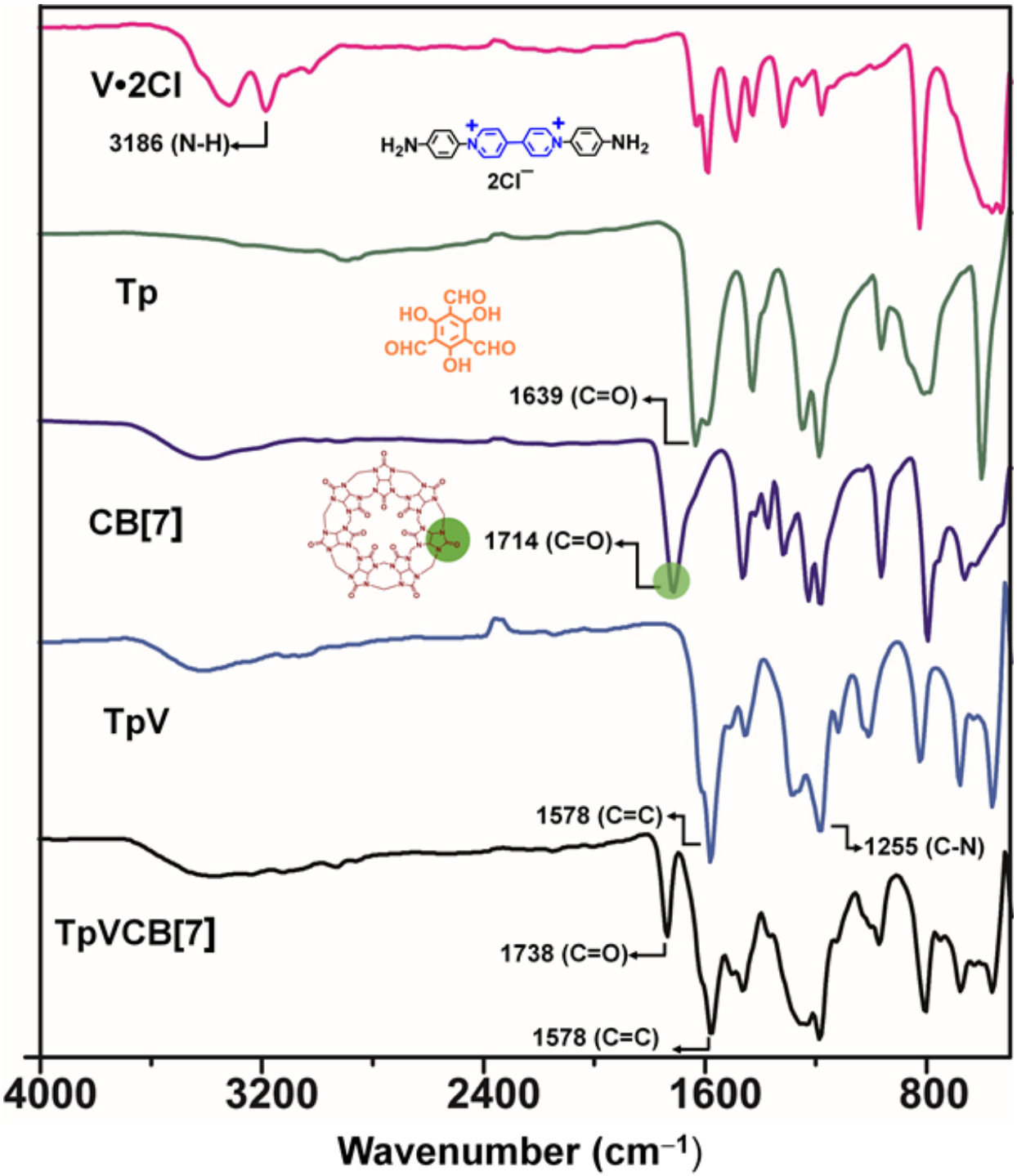

Supplementary Figure 1. Stacked FTIR spectra of precursors 1,1'-bis(2,4-dinitrophenyl)-[4,4'-bipyridine]-1,1'-diium dichloride (V•2Cl) (pink link), Phloroglucinol (Tp) (green line), Cucurbit[7]uril (CB[7]) (purple line), TpV (blue line) and TpVCB[7] (black line).

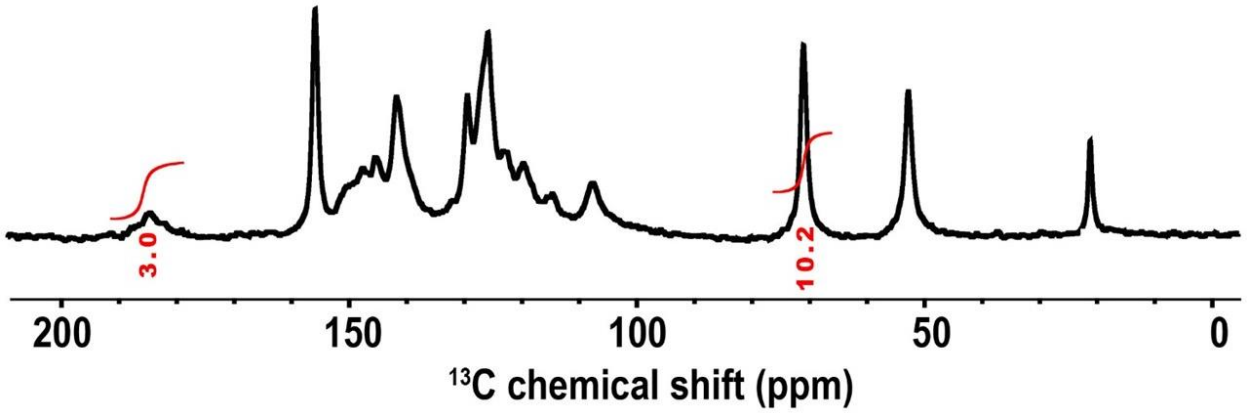

Supplementary Figure 2. ^{13}C quantitative spectrum of TpVCB[7].

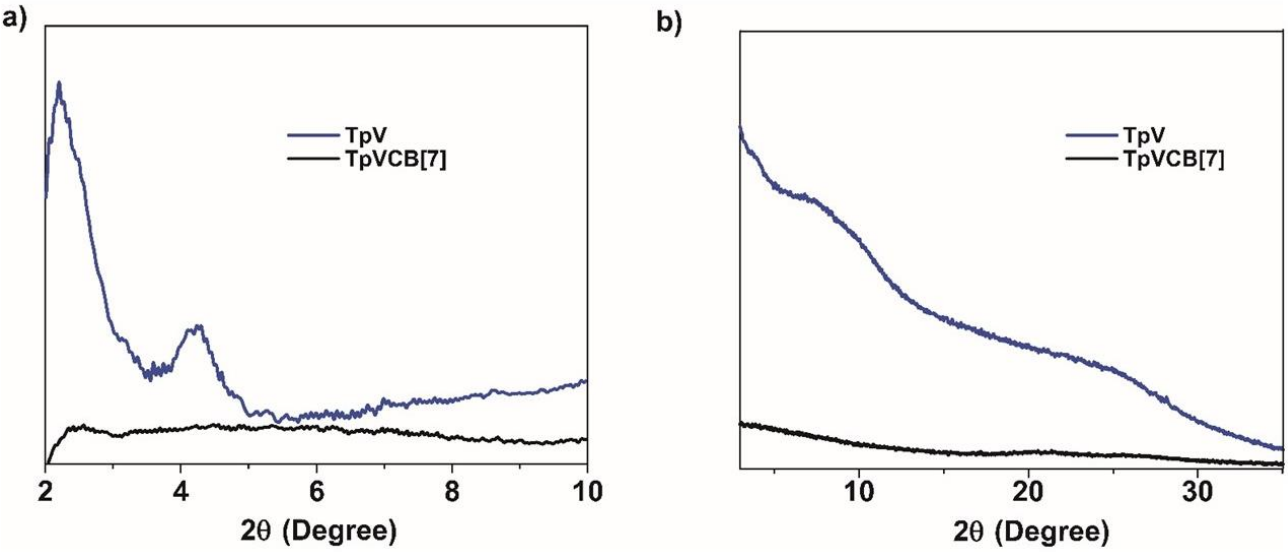

Supplementary Figure 3. Room temperature low angle PXRD (a) and wide angle (b) patterns of a) TpV (blue) and TpVCB[7] (black) .

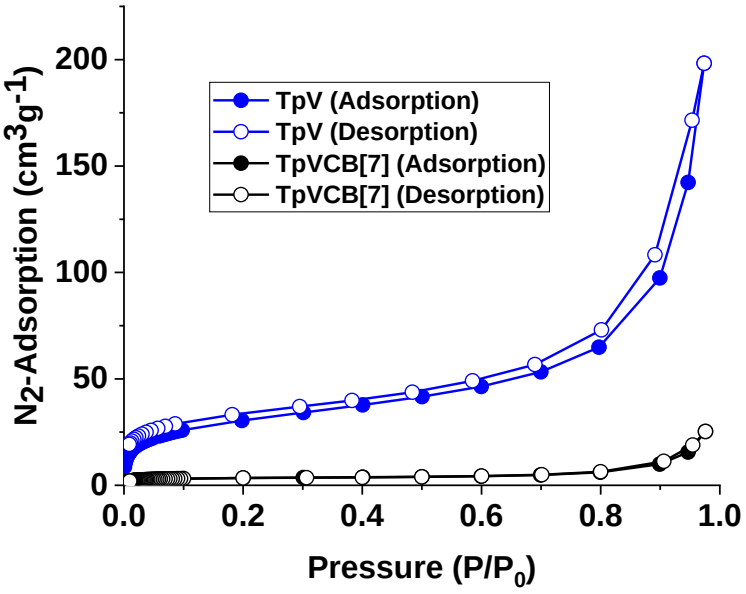

Supplementary Figure 4. N_2 adsorption isotherms of TpV and TpVCB[7] at 77 K.

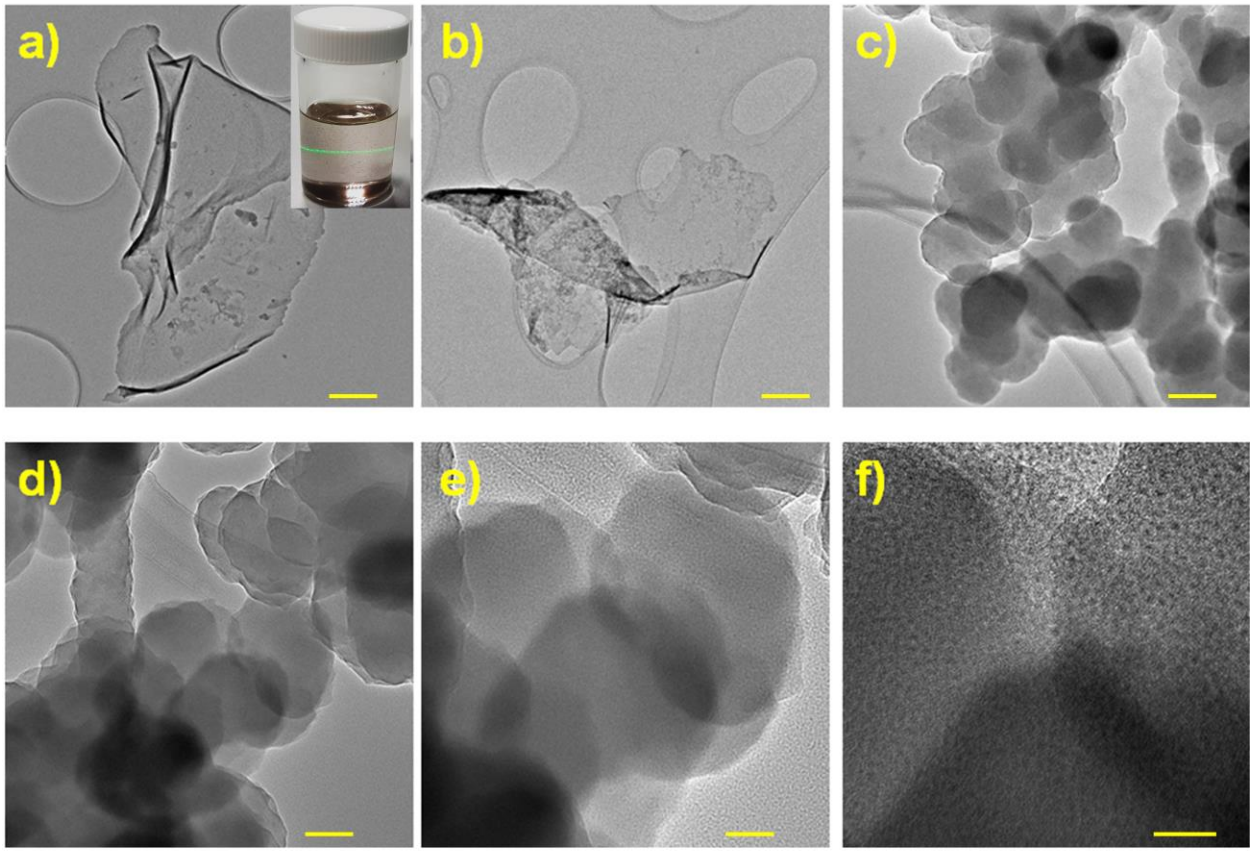

Supplementary Figure 5. HRTEM images (a, b, c, d, e, f) of TpV at different magnifications, transparent nature of nanosheets clearly indicating the formation of ultrathin structure. Inset in a) shows the nanosheets of TpV are well dispersed in ethanol and showed a Tyndall effect. Scale bar: a) 500nm, b) 500 nm, c) 200 nm, d) 100 nm, e) 50 nm and f) 20 nm.

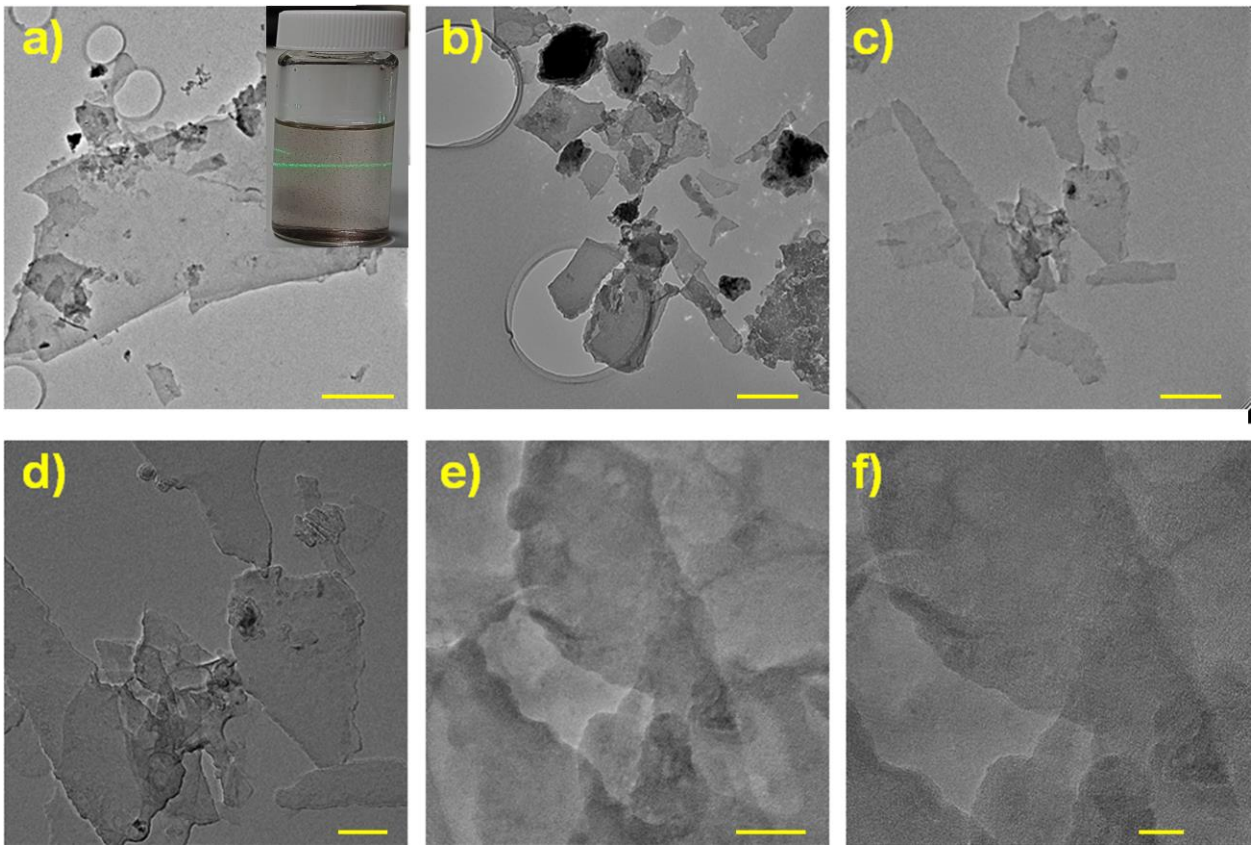

Supplementary Figure 6. HRTEM images (a, b, c, d, e, f) of TpVCB[7] at different magnifications, transparent nature of nanosheets clearly indicating the formation of ultrathin structure. Inset in a) shows the nanosheets of TpVCB[7] were well dispersed in ethanol and showed a Tyndall effect. Scale bar: a) 1μm, b) 500 nm, c) 500 nm, d) 200 nm, e) 50 nm and f) 50 nm.

Supplementary Figure 7. Stability of Tyndall effect, a-b) Tyndall effect for TpV and TpVCB[7]: The Tyndall effect could be observed for a long period of time, the solution remained stable even after two weeks.

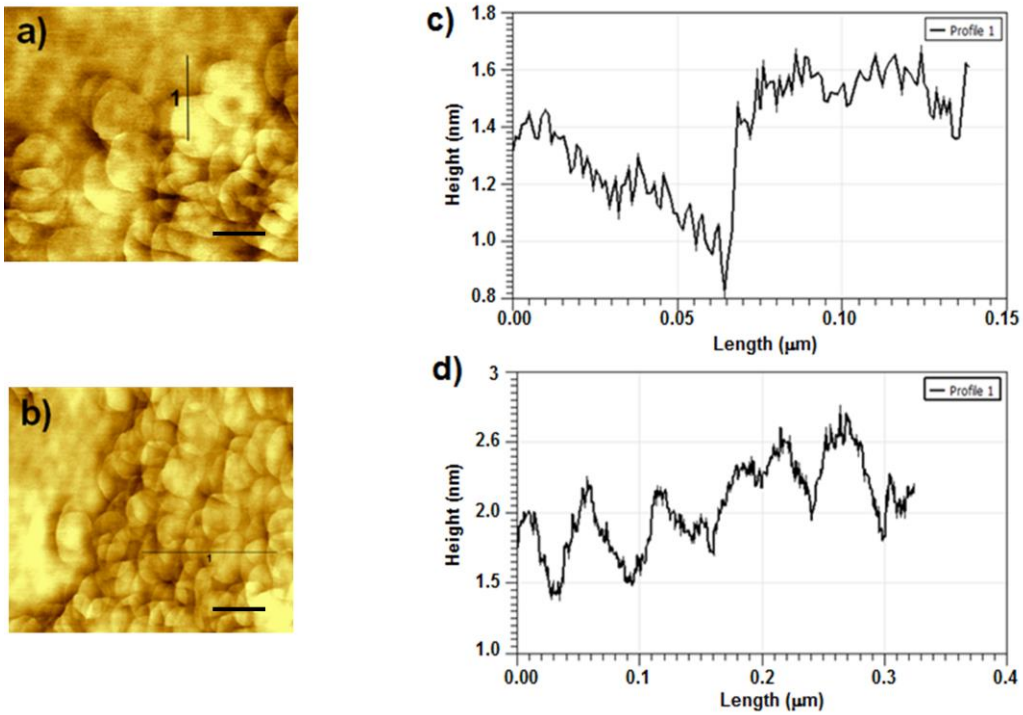

Supplementary Figure 8. AFM images of TpV (a-b) and (c-d) height profile diagrams of TpV. Scale bar: a-f) 200 nm.

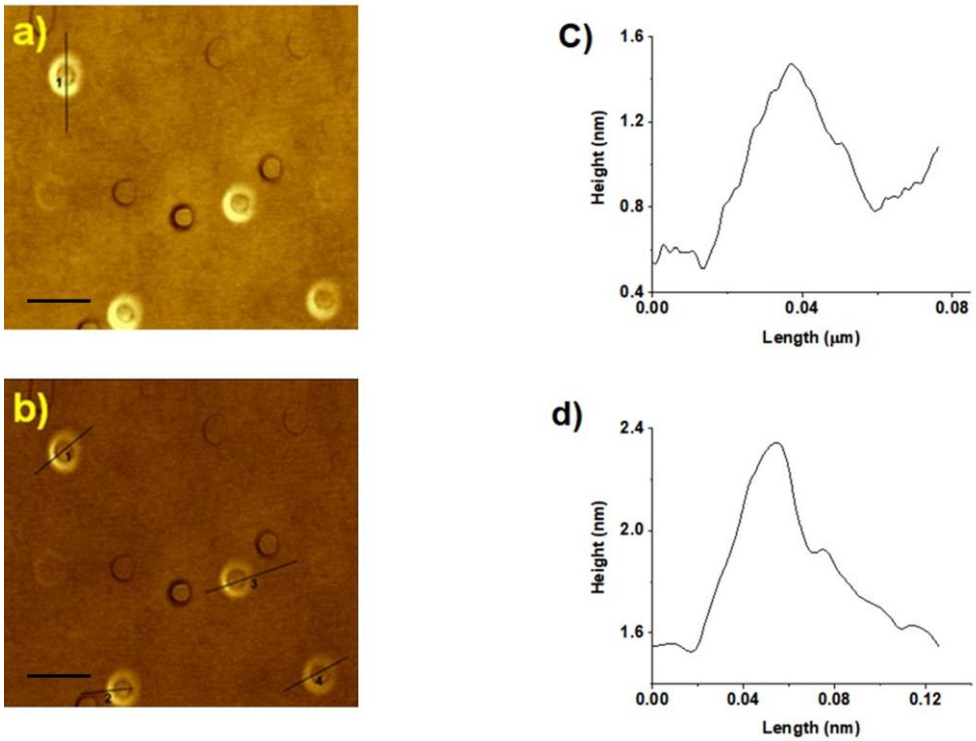

Supplementary Figure 9. AFM images of TpVCB[7] (a-b) and (c-d) height profile diagrams of TpVCB[7]. Scale bar: a-f) 500 nm.

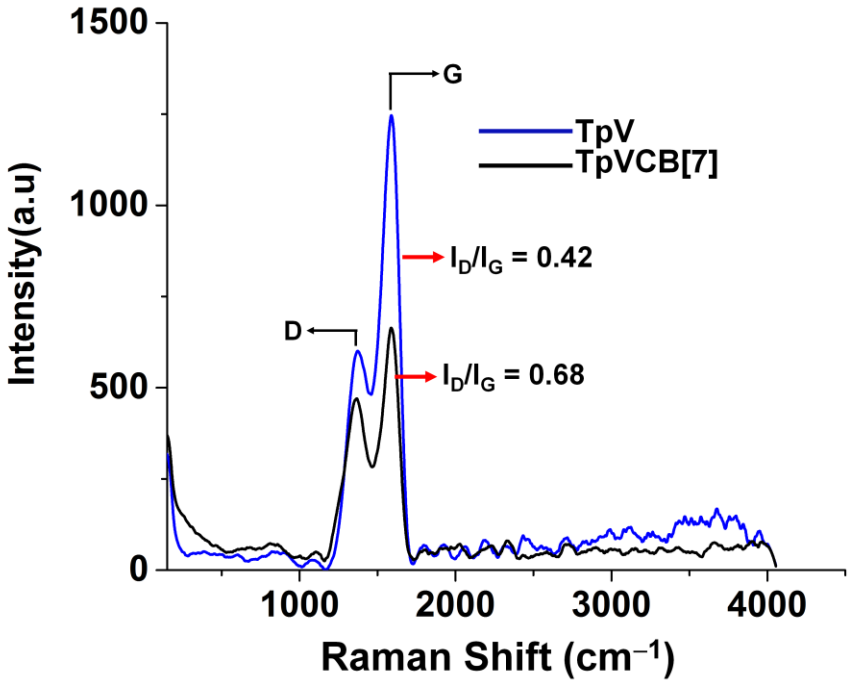

Supplementary Figure 10. Raman spectra of TpV and TpV CB[7].

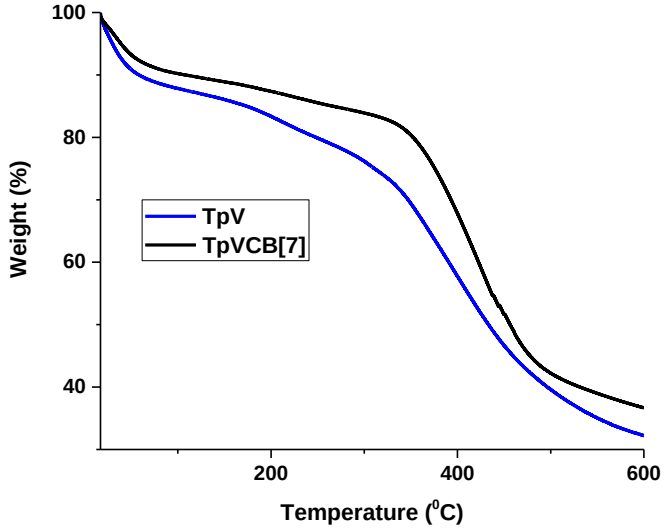

Supplementary Figure 11. TGA analysis of TpV and TpVCB[7].

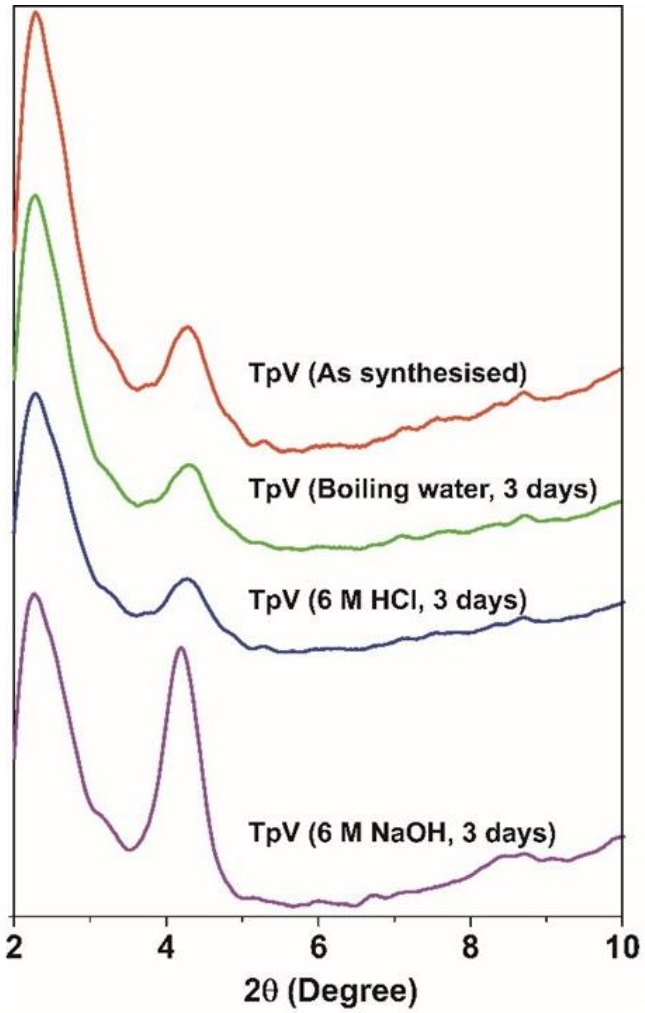

Supplementary Figure 12. Identical PXRD profiles suggest that the retention of characteristic peaks after keeping the TpV Film in boiling water, 6M hydrochloric acid and sodium hydroxide for 3 days.

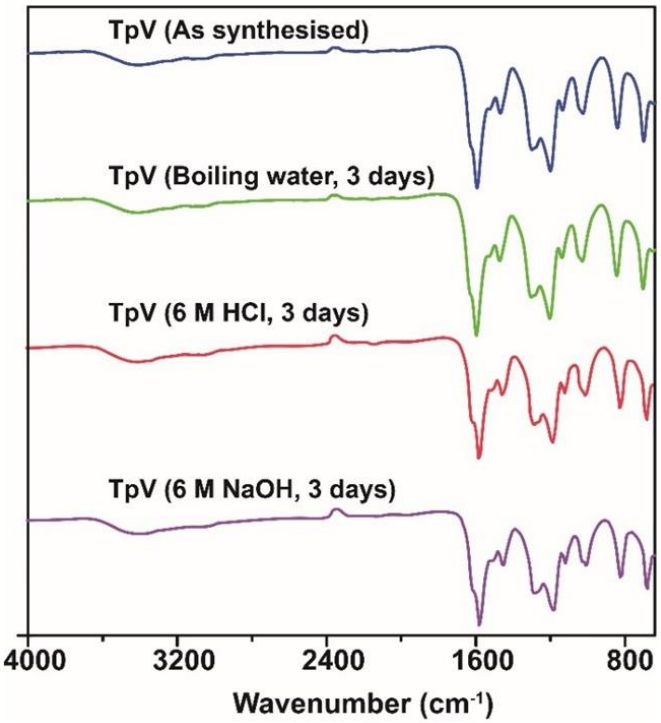

Supplementary Figure 13. FT-IR spectra reveal that the retention of characteristic peaks after keeping the TpV Film in boiling water, 6M hydrochloric acid and sodium hydroxide for 3 days.

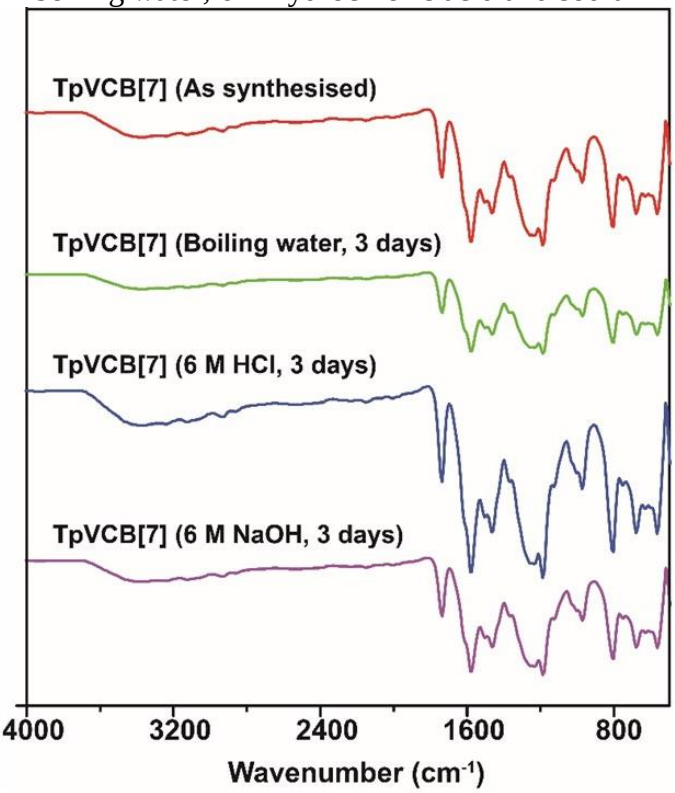

Supplementary Figure 14. FT-IR spectra reveal that the retention of characteristic peaks after keeping the TpVCB[7] Film in boiling water, 6M hydrochloric acid and sodium hydroxide for 3 days.

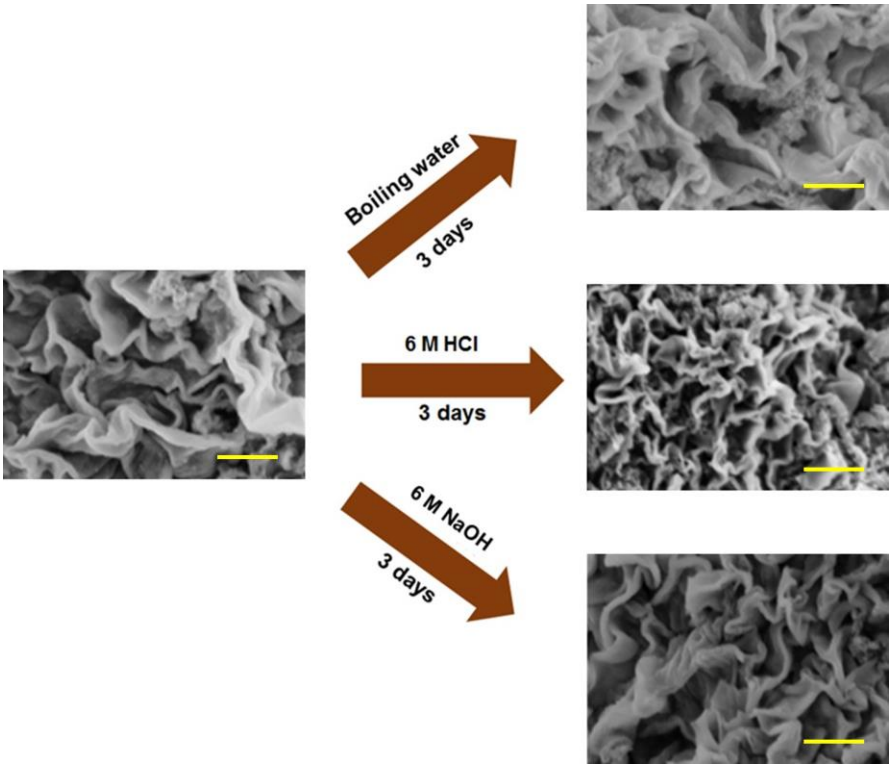

Supplementary Figure 15. SEM images of TpV after keeping the Film in boiling water, 6 M hydrochloric acid and sodium hydroxide for 3 days. Scale bar: a-f) 3 μm.

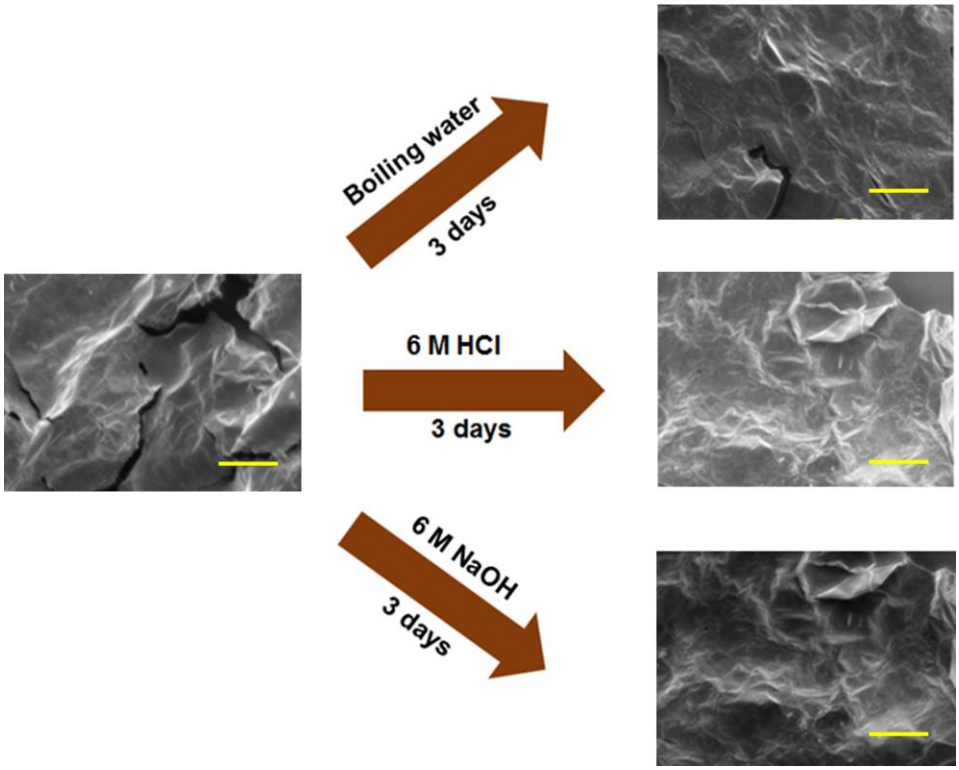

Supplementary Figure 16. SEM images of TpVCB[7] after keeping the Film in boiling water, 6 M hydrochloric acid and sodium hydroxide for 3 days. Scale bar: a-f) 50 μm.

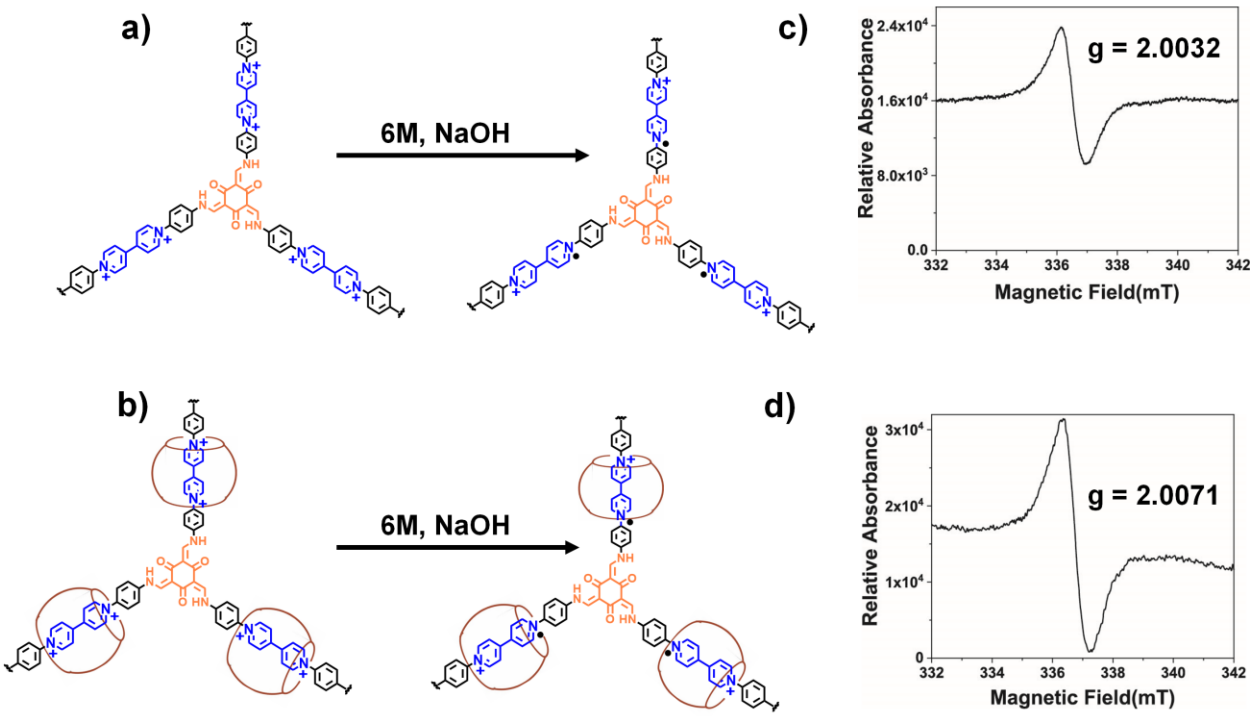

Supplementary Figure 17. Chemical structure of TpV (a), TpVCB[7] (b) and Solid-state EPR signals of TpV (c) and TpVCB[7] (d) after treatment with 6M of NaOH. The presence of thesignal confirms the radical character of both films in presence of base.

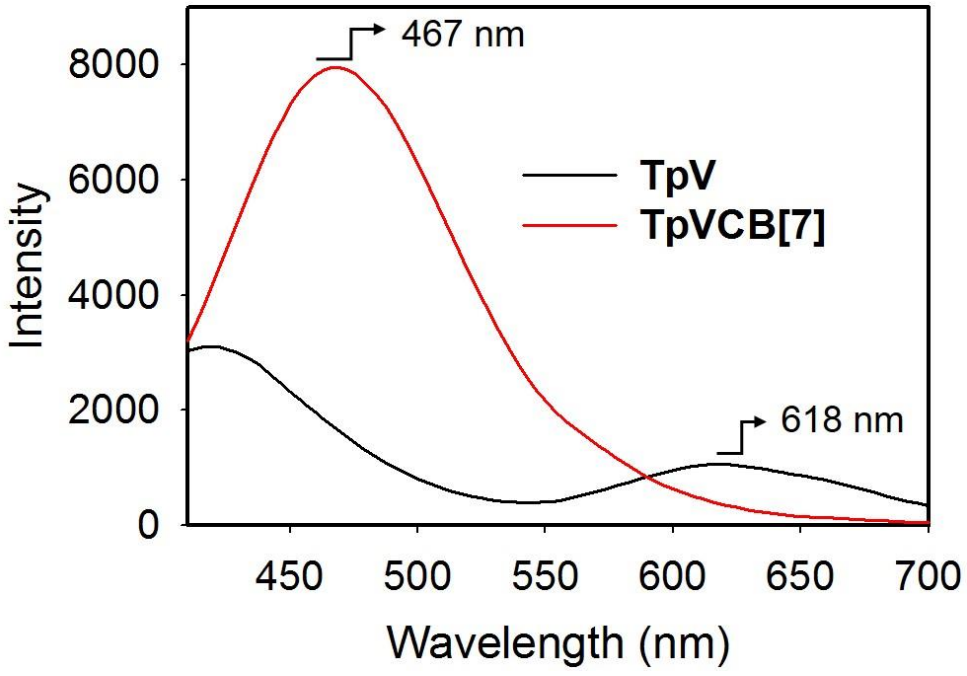

Supplementary Figure 18. Solid state luminescent spectra of TpV and TpVCB[7] recorded at room temperature with excitation wavelength 375 nm.

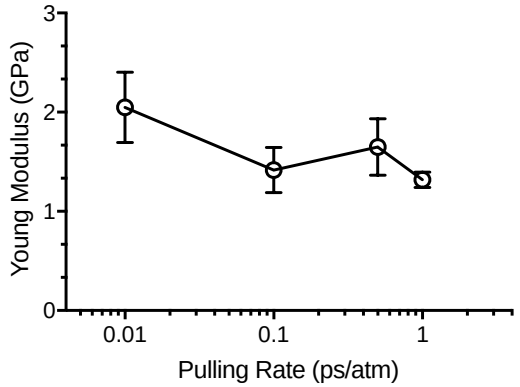

Supplementary Figure 19. Pulling rate dependence of the computed Young Modulus for TpV. The error bars represent the standard deviation of 3 experiments.

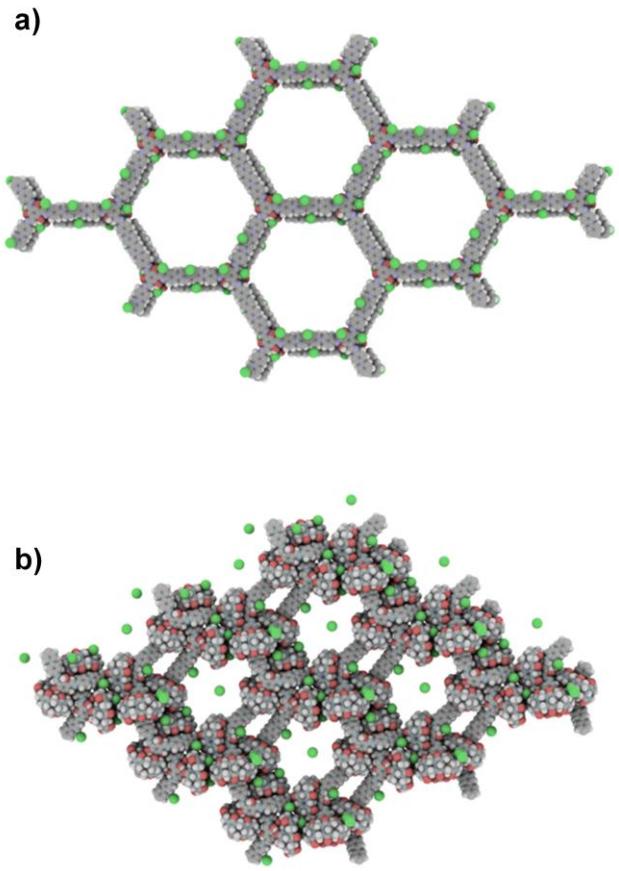

Supplementary Figure 20. Structural models of bilayers of TpV (a) and TpV CB[7] (b) from molecular dynamics simulations. **Black, C, N; White, Red, O; Green, Cl.**

Supplementary Note 1

To understand the mechanism of higher mechanical stability in TpVCB[7] we looked into the pairwise intermolecular energy between the components that constitutes the two Films. For TpV the two groups defined were Linker (L) and Cl- ions (Cl^-), while for TpVCB[7] we also added the Macrocycle (M) into analysis. We computed the average pairwise interaction between each group from equilibrium MD simulations using LAMMPS group module.

To compute the charge distribution of CB7 we used Quantum Mechanics calculations. NWChem 6.6 [1] is used for the computations. Starting from the minimized structure of the ring in the absence of the linker using Dreiding-x6 forcefield we optimized the geometry of the macrocycle using Hartree Fock theory with B3-LYP functional and 6-31G* basis set keeping all settings for minimization and convergence criteria default. Point charges were computed by fitting the electrostatic potential to point charges using ESP module followed by we computed the dipole moment.

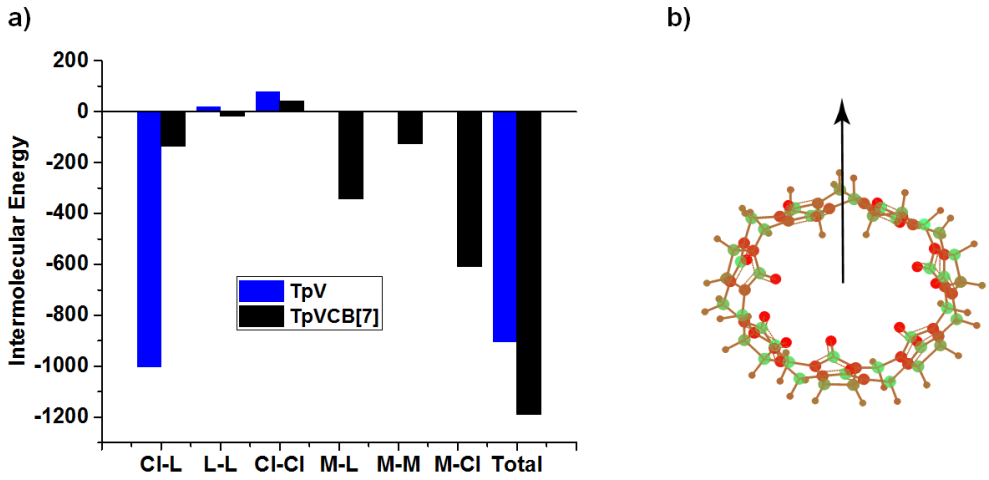

Supplementary Figure 21. a) Pairwise intermolecular energy between groups for TpV (blue) ans TpVCB[7] (orange). Pairwise interaction between different components defined as **M (**[CB7] macrocycle), **L** (polymer Linker), **Cl** (Chloride ions) are plotted. Values are averages over simulation data. **b)** Charge distribution of CB[7] shown in color map. Colors represent the electrostatic potential derived charges and ranges from +0.7 (green), to –0.7 (red). The charge distribution resulted in a dipole moment of 8.30 Debye in the direction of the arrow.

Supplementary Table 1

Table for the energy values of TpV and TpVCB[7]

(kcal/mol)	TpV	TpVCB[7]
Enthalpy H	–27	1825
$E_{potential}$	–335	849
$E_{coulombic}$	–820	–1953
E_{vdw}	131	–127

Supplementary References

1. M. Valiev, E.J. Bylaska, N. Govind, K. Kowalski, T.P. Straatsma, H.J.J. van Dam, D. Wang, J. Nieplocha, E. Apra, T.L. Windus, W. A. d. Jong, NWChem: a comprehensive and scalable open-source solution for large scale molecular simulations. *Comput. Phys. Commun.* **181**, 1477-1489 (2010).